Colloid Polym Sci (2004) 282: 1392–1402
DOI 10.1007/s00396-004-1079-2

ORIGINAL CONTRIBUTION

H. Iyota
R. Krustev
H.-J. Müller

Thermodynamic studies on thin liquid films. II. Foam film stabilized by decyl methyl sulfoxide

Received: 16 June 2003
Accepted: 24 December 2003
Published online: 6 May 2004

H. Iyota (✉) · R. Krustev · H.-J. Müller
Max Planck Institute of Colloids and Interfaces, Am Mühlenberg 1, D-14476 Golm, Germany
E-mail: iyota@k-kentan.ac.jp
Tel.: +81-99-220-1111
Fax: +81-99-220-1115

Present address: H. Iyota
Kagoshima Prefectural College, 1-52-1 Shimoishiki, 890–0005 Kagoshima, Japan

Abstract Thermodynamic equations in Part I of this series were extended so as to be applicable to electrolyte mixtures and the resultant equations were applied to the experimental results of a NaCl-decyl methyl sulfoxide (DeMS) mixture. Film thickness and contact angle of the black foam film stabilized by DeMS were measured as a function of the total molality of NaCl and DeMS at constant mole fraction of DeMS in the mixture under constant disjoining pressure. Newton black film was observed only above a certain DeMS concentration and the phase transition between common black and Newton black films took place twice as NaCl concentration increased at constant DeMS concentration. The surface densities of NaCl and DeMS at the film surface and the differences in the surface densities between the adsorbed films at the film surface and bulk one coexisting at equilibrium were numerically evaluated by applying the thermodynamic equations to the film tension obtained from the contact angle. The film states and phase transitions were clarified in terms of the film thickness and surface densities.

Keywords Equivalent film thickness · Contact angle and film tension · Phase transition in black foam film · Mixture of NaCl and non-ionic surfactant · Thermodynamics of thin liquid films

Introduction

It is essential to obtain thermodynamic quantities of thin liquid films to clarify the structure and properties of the films. Surface excess of component i per unit area (surface density) at the film surface of a plane-parallel foam film and the difference in surface density between the film surface and meniscus are usually evaluated by applying

$$\left(\partial\gamma^{\mathrm{f}}/\partial\mu_i\right)_{T,\Pi,\mu_j} = -2\Gamma_i \tag{1}$$

and

$$\left[\partial\left(\gamma^{\mathrm{f}} - 2\gamma\right)/\partial\mu_i\right]_{T,\Pi,\mu_j} = -2\left(\Gamma_i - \Gamma_i^{\mathrm{G}}\right) \tag{2}$$

to the film tension γ^{f} and the difference between the film tension and surface tension γ measured at constant temperature under atmospheric pressure, respectively [1, 2, 3, 4, 5, 6]. Here Γ_i denotes the surface density of solute component i at the film surface based on the surface excess convention and Γ_i^G the one at the meniscus based on the Gibbs convention, and subscript μ_j means that all the chemical potentials of solutes except μ_i are kept constant. However, taking into account the fact that experiments on a plane-parallel film are normally conducted under constant pressure in the phase surrounding both sides of the film, Eq. 1 and Eq. 2 are approximate ones and the exact equations (see Appendix I and [7]) are:

$$\left(\partial\gamma^{\mathrm{f}}/\partial\mu_i\right)_{T,p,\Pi,\mu_j} = -2\left[\Gamma_i - \Gamma_a\left(c_l^{\mathrm{L}}c_i^{\mathrm{A}} - c_l^{\mathrm{A}}c_i^{\mathrm{L}}\right)/\left(c_l^{\mathrm{L}}c_a^{\mathrm{A}} - c_l^{\mathrm{A}}c_a^{\mathrm{L}}\right)\right] \quad (3)$$

and

$$\left[\partial\left(\gamma^{\mathrm{f}} - 2\gamma\right)/\partial\mu_i\right]_{T,p,\Pi,\mu_j} = -2\left[\left(\Gamma_i - \Gamma_i^{\mathrm{G}}\right) - \left(\Gamma_a - \Gamma_a^{\mathrm{G}}\right)\left(c_l^{\mathrm{L}}c_i^{\mathrm{A}} - c_l^{\mathrm{A}}c_i^{\mathrm{L}}\right)/\left(c_l^{\mathrm{L}}c_a^{\mathrm{A}} - c_l^{\mathrm{A}}c_a^{\mathrm{L}}\right)\right] \quad (4)$$

where c_i is the concentration of component i expressed in number of moles per unit volume and subscripts a and l indicate the solvents of the ambient phases A and L, respectively. On the other hand, the corresponding equations can be obtained from Eqs. 6, 49 and 65 in Part I of this series [8],

$$\left(\partial\gamma^{\mathrm{f}}/\partial\mu_i\right)_{T,p,\Pi,\mu_j} = -2\Gamma_i^{\mathrm{F}} \quad (5)$$

and

$$\left[\partial\left(\gamma^{\mathrm{f}} - 2\gamma\right)/\partial\mu_i\right]_{T,p,\Pi,\mu_j} = -2\left(\Gamma_i^{\mathrm{F}} - \Gamma_i^{\mathrm{H}}\right), \quad (6)$$

employing the new convention for the film and the Hansen convention for the interface. Hence the measurements of the film tension and the difference between film tension and surface tension at constant temperature and disjoining pressure under atmospheric pressure don't give Γ_i and $\Gamma_i - \Gamma_i^{\mathrm{G}}$ but Γ_i^{F} and $\Gamma_i^{\mathrm{F}} - \Gamma_i^{\mathrm{H}}$.

de Feijter et al. evaluated the difference in surface excess per unit area and the corresponding entropy between the film surface and adjacent meniscus based on the surface excess convention for the foam film stabilized by sodium dodecyl sulfate (SDS) from a contact angle measurement [4]. However, their measurement (diffraction method for a vertical film and expansion method for a horizontal one) was not conducted at constant disjoining pressure, which is inconsistent with the thermodynamic requirements of the convention. In Part I, we have developed thermodynamic equations based on the new convention, applicable to the film tension as a function of temperature, pressure, disjoining pressure, and the molalities of solutes. The present study aims to extend the thermodynamic equations in Part I so as to be applicable to electrolyte mixtures and apply the resulting equations to a NaCl-decyl methyl sulfoxide (DeMS) mixture. Contact angle between the film and the adjacent meniscus is measured as a function of the total molality of NaCl and DeMS at constant mole fraction of DeMS in the total solutes at 298.15 K, and constant disjoining pressure under atmospheric pressure, and then the thermodynamic equations are applied to the film tension obtained from the surface tension previously measured [9] and the contact angle.

Equivalent thickness of thin liquid films has been interferometrically measured as a function of the concentration of added salt to identify film states and transition in a film [10, 11, 12, 13]. Clunie [14] and Ingram [15] measured the thickness and tension difference for DeMS foam films at the CMC and found the thickness transition at higher NaCl concentration. In the present study, equivalent fim thickness was also measured for the DeMS film as a function of the total molality of NaCl and DeMS and the mole fraction of DeMS in the mixture to investigate the effect of DeMS concentration as well as the one of NaCl concentration on the film state and thickness transition.

Combination of the contact angle and thickness measurements will clarify the relationship between the film thickness and thermodynamic quantities of the film surface, the film thickness at which the interaction between surfaces in the film begins to take place, and the relationship between the variations in contact angle and thickness at the transition in the film.

Theoretical

Let us consider a thin liquid film formed from the solution of a binary mixture of electrolytes having no common ions: electrolyte 1 dissociates into $\nu_{1,\mathrm{a}}a$-ions and $\nu_{1,\mathrm{c}}c$-ions and electrolyte 2 into $\nu_{2,\mathrm{b}}b$-ions and $\nu_{2,\mathrm{d}}d$-ions. Assuming the solution to be ideal and the electrolytes to be strong ones, we can rewrite Eq. 6 in Part I of this series in the form:

$$\mathrm{d}\gamma^{\mathrm{f}} = -s^{\mathrm{f}}\mathrm{d}T + v^{\mathrm{f}}\mathrm{d}p + v^{\mathrm{L}}\mathrm{d}\Pi - \Gamma_a^{\mathrm{f}}\mathrm{d}\mu_a - \Gamma_c^{\mathrm{f}}\mathrm{d}\mu_c - \Gamma_b^{\mathrm{f}}\mathrm{d}\mu_b - \Gamma_d^{\mathrm{f}}\mathrm{d}\mu_d \quad (7)$$

where μ_j is the chemical potential of j-ion and Γ_j^{F} is the corresponding film density. Substituting differentials of the chemical potentials of ions into Eq. 7 and rearranging the resulting equation leads to:

$$\mathrm{d}\gamma^{\mathrm{f}} = -\Delta s^{\mathrm{f}}\mathrm{d}T + \Delta v^{\mathrm{f}}\mathrm{d}p + \tau^{\mathrm{f}}\mathrm{d}\Pi - \left(\nu_1 RT\Gamma_1^{\mathrm{f}}/m_1\right)\mathrm{d}m_1 - \left(\nu_2 RT\Gamma_2^{\mathrm{f}}/m_2\right)\mathrm{d}m_2 \quad (8)$$

where m_1 and m_2 are the molalities of electrolytes 1 and 2, respectively and ν_1 and ν_2 denote

$$\nu_1 = \nu_{1,a} + \nu_{1,c},\ \nu_2 = \nu_{2,b} + \nu_{2,d} \quad (9)$$

Here, film densities of electrolytes 1 and 2 are defined by

$$\Gamma_1^{\mathrm{f}} = \left(\Gamma_a^{\mathrm{f}} + \Gamma_c^{\mathrm{f}}\right)/\nu_1,\ \Gamma_2^{\mathrm{f}} = \left(\Gamma_b^{\mathrm{f}} + \Gamma_d^{\mathrm{f}}\right)/\nu_2 \quad (10)$$

and thermodynamic quantity change Δy^{f} associated with adsorption at film interfaces by

$$\Delta y^{\mathrm{f}} = y^{\mathrm{f}} - \Gamma_a^{\mathrm{f}}y_a - \Gamma_c^{\mathrm{f}}y_c - \Gamma_b^{\mathrm{f}}y_b - \Gamma_d^{\mathrm{f}}y_d,\ \ (y = s, v) \quad (11)$$

and thermodynamic film thickness τ^{f} by

$$\tau^{\mathrm{f}} = v^{\mathrm{L}} + \Gamma_a^{\mathrm{f}}v_a + \Gamma_c^{\mathrm{f}}v_c + \Gamma_b^{\mathrm{f}}v_b + \Gamma_d^{\mathrm{f}}v_d. \quad (12)$$

Hence Δy^{f},τ^{f}, Γ_1^{f}, and $\Gamma_2^{f}$are related toγ^{f} by

$$\Delta s^{f} = -\left(\partial\gamma^{f}/\partial T\right)_{p,\Pi,m_1,m_2} \tag{13}$$

$$\Delta v^{f} = \left(\partial\gamma^{f}/\partial p\right)_{T,\Pi,m_1,m_2}, \tag{14}$$

$$\tau^{f} = \left(\partial\gamma^{f}/\partial\Pi\right)_{T,P,m_1,m_2}, \tag{15}$$

$$\Gamma_1^{f} = -(m_1/v_1RT)\left(\partial\gamma^{f}/\partial m_1\right)_{T,p,\Pi,m_2}, \tag{16}$$

and

$$\Gamma_2^{f} = -(m_2/v_2RT)\left(\partial\gamma^{f}/\partial m_2\right)_{T,p,\Pi,m_1}. \tag{17}$$

The corresponding energy and enthalpy changes are given by the same equations as Eq. 47 and 48 in Part I, respectively. On the other hand, Eq. 49 for interfacial tension in Part I [8] is rewritten in the form

$$\begin{aligned} d\gamma_K = &-\Delta s_K dT + \Delta v_K dp + \left(v_K^{H,K} - \Delta v_K\right)d\Pi \\ &- \left(v_1RT\Gamma_1^{H,K}/m_1\right)dm_1 \\ &- \left(v_2RT\Gamma_2^{H,K}/m_2\right)dm_2, \ (K = A, B). \end{aligned} \tag{18}$$

Hence, combination of Eq. 8 with Eq. 18 yields the differences in the thermodynamic quantities between the film interface and the adjacent meniscus:

$$\Delta s^{f} - \Delta s_A - \Delta s_B = -\left[\partial\left(\gamma^{f} - \gamma_A - \gamma_B\right)/\partial T\right]_{p,\Pi,m_1,m_2}, \tag{19}$$

$$\Delta v^{f} - \Delta v_A - \Delta v_B = \left[\partial\left(\gamma^{f} - \gamma_A - \gamma_B\right)/\partial p\right]_{T,\Pi,m_1,m_2}, \tag{20}$$

$$\begin{aligned} &\tau^{f} - v_A^{H,A} - v_B^{H,B} + \Delta v_A + \Delta v_B \\ &\quad = \left[\partial\left(\gamma^{f} - \gamma_A - \gamma_B\right)/\partial\Pi\right]_{T,p,m_1,m_2}, \end{aligned} \tag{21}$$

$$\begin{aligned} &\Gamma_1^{f} - \Gamma_1^{H,A} - \Gamma_1^{H,B} \\ &\quad = -\left(m_1/v_1RT\right)\left[\partial\left(\gamma^{f} - \gamma_A - \gamma_B\right)/\partial m_1\right]_{T,p,\Pi,m_2}, \end{aligned} \tag{22}$$

and

$$\begin{aligned} &\Gamma_2^{f} - \Gamma_2^{H,A} - \Gamma_2^{H,B} \\ &\quad = -\left(m_2/v_2RT\right)\left[\partial\left(\gamma^{f} - \gamma_A - \gamma_B\right)/\partial m_2\right]_{T,p,\Pi,m_1}. \end{aligned} \tag{23}$$

The corresponding equations for the differences in energy and enthalpy are the same as Eqs. 62 and 63 in Part I, respectively.

Materials and methods

NaCl and DeMS are the same samples as those used in the previous study [9]. Solutions were prepared from doubly-distilled water, purified using a Millipore-Q apparatus [16].

Equivalent film thickness was interferometrically measured for microscopic horizontal foam films formed in the circular glass tube of a Scheldko-type ring cell [11, 16]. The refractive index of NaCl solutions was used to calculate the equilibrium thickness because the concentration of DeMS is very small. The contact angle between the film and the adjacent meniscus was measured by the expansion technique, and for small contact angle below 0.5° by the topographic one [16, 17, 18]. Experimental errors inherent in the measurements were less than 0.2 nm for the thickness measurement, 0.1° for the expansion technique and 0.13° for the topographic one. The contact angle values obtained by the two techniques for the same solution were in good agreement within the errors.

The glass ring cell filled with a sample solution was left for 1 h in a closed metal container, thermostatted to attain thermal equilibrium with the system and the atmosphere surrounding the film saturated with the solution vapor. The capillary pressure in the film system, and hence the disjoining pressure Π, can be calculated by the equation

$$\Pi = (2\gamma/R)\left[1 - (r/R)^2\right]^{-1}, \tag{24}$$

where r and R are the initial film radius and the tube radius of the ring cell respectively, and γ is the surface tension of the film-forming solution. In Eq. 24, the wetting angle between the meniscus and the finely furrowed inner surface of the glass tube was assumed to be zero [19]. It is conventional to measure film thickness and contact angle at constant r with a ring cell of constant R even when the concentrations of surfactant and NaCl are changed. Then, Π varies with the concentrations because the surface tension γ of the solution changes with the concentrations. Therefore, in the present experiment, to keep disjoining pressure Π constant, we changed r (0.2 mm–0.8 mm) and R ($2R = 3.5$, 4.0, 4.5, 5.0 mm) so that the changes in r and R compensate the variation of surface tension with the molalities of NaCl and DeMS (see Appendix II). The surface tension of solutions of a NaCl-DeMS mixture measured in the previous study [9] was used.

Stable black films were obtained at concentrations above about one-half of the CMC of DeMS. All the measurements were conducted at 298.15 K and $\Pi = 30$ Pa under atmospheric pressure. Temperature was kept constant within 0.1 °K and the error in the disjoining pressure was less than 0.4 Pa.

Results and discussion

Equivalent film thickness and contact angle as a function of the total molality and the mole fraction of DeMS

According to the thermodynamic treatment of surfactant mixture applied to inorganic salt-surfactant

mixtures [20], the total molality $\hat{m}$ of NaCl and DeMS and the mole fraction $\hat{X}_2$ of DeMS in the mixture,

$$\hat{m} = 2m_1 + m \tag{25}$$

and

$$\hat{X}_2 = m_2/\hat{m} \tag{26}$$

were taken as the experimental variables at constant temperature, pressure, and disjoining pressure. Figure 1 shows the equivalent film thickness h_w as a function of $\hat{m}$ at constant $\hat{X}_2$. We see a sudden decrease in h_w after a monotonous decrease in h_w with increasing $\hat{m}$. Judging from the finding that the h_w just before the jump depends on $\hat{X}_2$ and the one after it doesn't, the jump is ascribed to the phase transition from common black to Newton black films. The phase transition is not observed at $\hat{X}_2$ larger than 0.8 and lower than 0.014, where NaCl concentration is very small in the former and very high in the latter. In the thinning process of a film to the Newton black film in the vicinity of the transition, black spot formation took place twice: common black film whose thickness is about 10 nm first appeared after black spot formation in a thick film, and then the second spot of a Newton black film appeared in the common black film and spread over the film. Figure 2 shows the contact angle θ versus $\hat{m}$ curve at constant $\hat{X}_2$. θ increases with increasing $\hat{m}$ and the θ versus $\hat{m}$ curve breaks at the $\hat{m}$ where h_w shows a sudden change, denoted by the arrow on the curve. Therefore we can say that the phase transition in the film is accompanied by the jump in h_w and the discontinuity in θ. In Fig. 1 and Fig. 2, it is indicated that θ is zero when h_w is larger than about 20 nm and h_w decreases and θ increases as $\hat{m}$ increases. In the region of Newton black film at higher $\hat{m}$, θ increases greatly with increasing $\hat{m}$ whereas h_w is constant. It is notable that the θ of DeMS foam film is less than 2°, and much smaller than the corresponding one of ionic surfactants [18, 21].

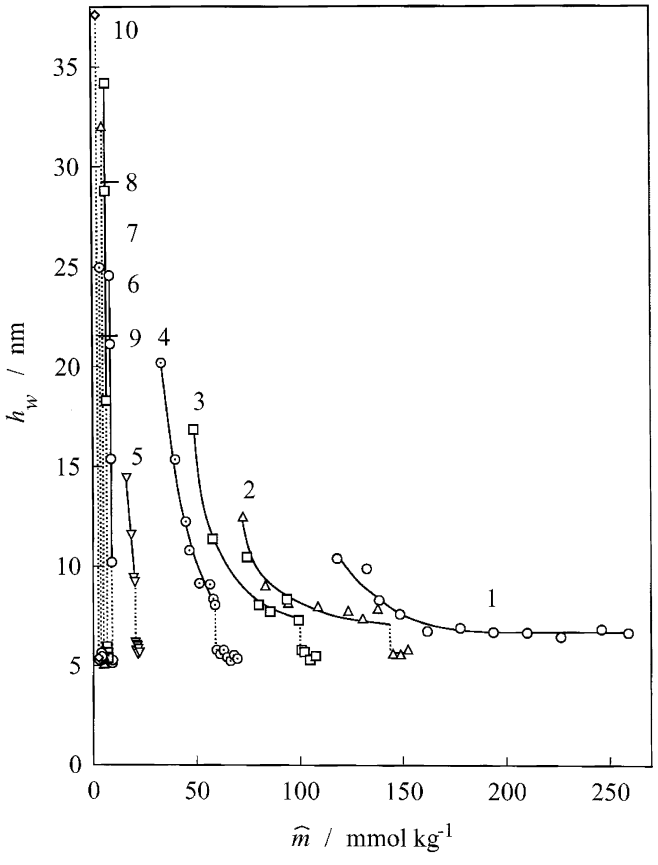

Fig. 1 Equivalent film thickness (h_w) vs. total molality ($\hat{m}$) curves at constant composition. *1* Mole fraction $\hat{X}_2 = 0.00772$, *2* 0.01379, *3* 0.01810, *4* 0.03015, *5* 0.09173, *6* 0.2150, *7* 0.2884, *8* 0.3817, *9* 0.4984, *10* 0.7999

Equivalent film thickness and contact angle as a function of NaCl concentration

The h_w and θ values at a given molality m_2 of DeMS read from Fig. 1 and Fig. 2 are plotted as a function of the molality m_1 of NaCl in Fig. 3a and b, respectively. Here, m_1 and m_2 are given by rewriting Eq. 25 and Eq. 26:

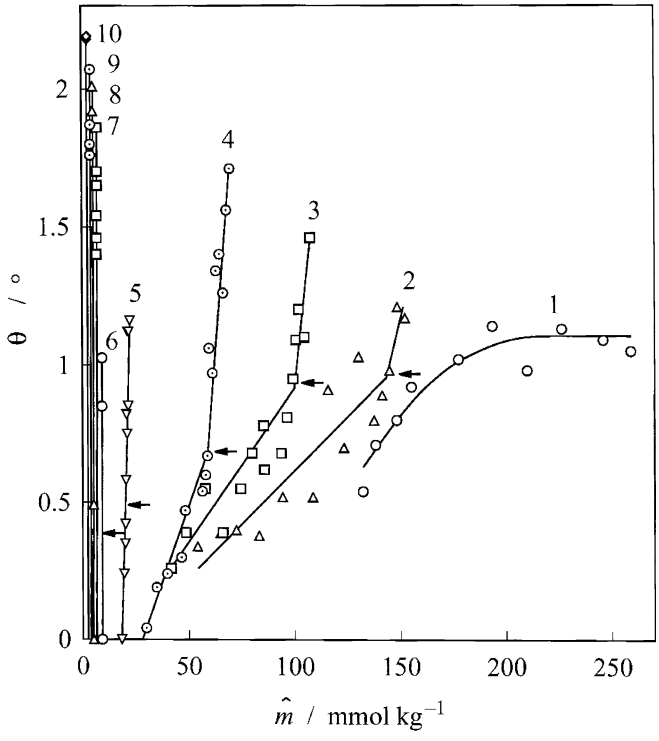

Fig. 2 Contact angle θ vs. total molality curves at constant composition. *1* $\hat{X}_2 = 0.00772$, *2* 0.01379, *3* 0.01810, *4* 0.03015, *5* 0.09173, *6* 0.2150, *7* 0.2884, *8* 0.3817, *9* 0.4984, *10* 0.7999

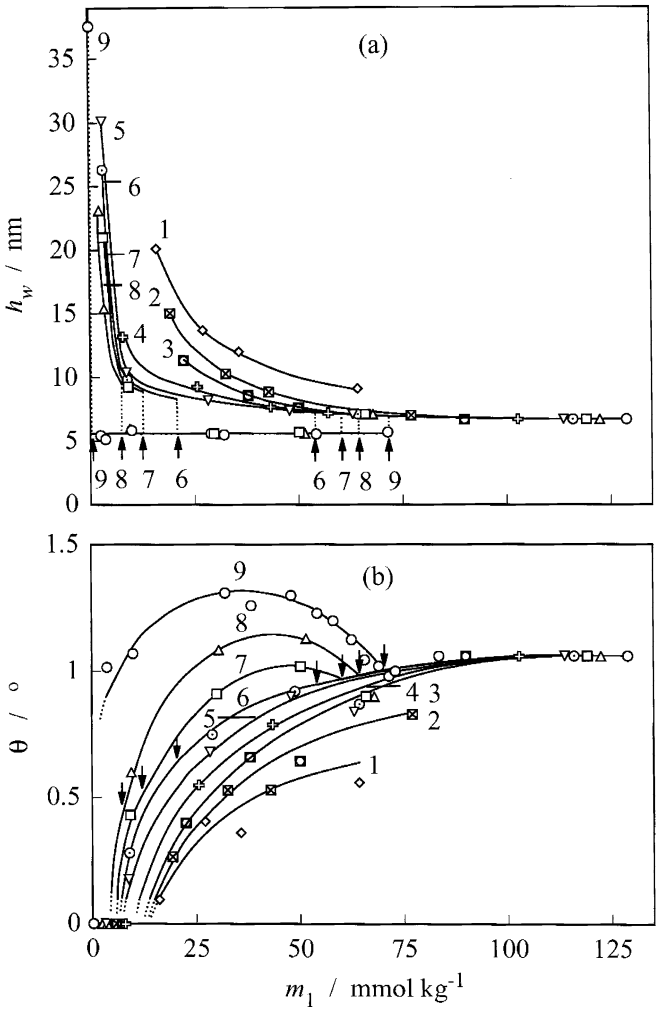

Fig. 3a, b Equivalent film thickness vs. molality of NaCl curves (**a**), and contact angle vs. molality of NaCl curves at constant decyl methyl sulfoxide (DeMS) concentration (**b**): *1* $m_2 = 1.0$ mmol kg^{-1}, *2* 1.2 mmol kg^{-1}, *3* 1.4 mmol kg^{-1}, *4* 1.6 mmol kg^{-1}, *5* 1.765 mmol kg^{-1}, *6* 1.8 mmol kg^{-1}, *7* 1.85 mmol kg^{-1}, *8* 1.9 mmol kg^{-1}, *9* 2.0 mmol kg^{-1}

$$m_1 = \frac{1}{2}\hat{m}\left(1 - \hat{X}_2\right) \tag{27}$$

and

$$m_2 = \hat{m}\hat{X}_2. \tag{28}$$

The h_w and θ values measured as a function of m_1 at $m_2 = 2$ mmol kg^{-1} (CMC of DeMS) are also presented. The h_w versus m_1 curve at larger m_2 shows two phase transitions indicated by the arrows for each m_2; as m_1 increases, h_w gets down to 5.6 nm at the first transition and returns to a lager value at the second one, that is, the first transition is from the common black to Newton black films and the second one from the Newton black to common black ones. It is worth noting that the h_w of the Newton black film is 5.6 nm and independent both of m_1 and m_2. The first transition is similar to those observed for ionic surfactants. However, the NaCl concentration at which the transition occurs is two orders of magnitude smaller for DeMS than for ionic surfactants [22], and depends on the DeMS concentration. The two transitions at a given m_2 come closer as m_2 decreases. Clunie [14] and Ingram [15] missed the first transition because the DeMS concentration was fixed at the CMC in their experiment and the NaCl concentration at which the transition takes place is very small at the CMC, as shown in Fig. 3a. The second transition is characteristic of DeMS and has not been observed for ionic surfactants. The jump in h_w, similar to that at the second transition, is also observed for other nonionic surfactants [13] and phospholipids in the presence of $CaCl_2$ [23, 24, 25]. It can be seen from Fig. 3b that the θ versus m_1 curve at higher m_2 has two breaks indicating the phase transitions in the film designated by the arrows, and the curves converge at higher m_1.

Equivalent film thickness and contact angle as a function of DeMS concentration

Dependence of film properties on surfactant concentration has been reported less than that on inorganic salt concentration [26]. Figure 4a and b show the h_w and θ at a given m_1 taken from Fig. 3, as a function of m_2, respectively. We see h_w decreases with increasing m_2 and phase transition takes place from the common black to Newton black films except at very high m_1. On the other hand, θ increases with increasing m_2 and the θ versus m_2 curve changes its slope sharply at the phase transition. Thus the film thickness, contact angle, and phase transition in the film significantly depend on DeMS concentration as well as NaCl concentration.

The molality $m_2$at the phase transition, m_2^{eq}, obtained from the transition point on the h_w versus $\hat{m}$ curve in Fig. 1, is plotted against m_1 in Fig. 5. The m_2^{eq} versus m_1 curve has a minimum at $m_2^{eq} = 1.765$ mmol kg^{-1}, that is, Newton black film can be observed only at m_2 above the critical molality, 1.765 mmol kg^{-1}, of DeMS.

Difference between film tension and surface tension as a function of NaCl and DeMS concentrations

Difference $\gamma^f - 2\gamma$ between the film tension and the surface tension of the film-forming solution coexisting in equilibrium with the film is obtained by substituting the θ in Fig. 3b and Fig. 4b and γ values into

$$\gamma^f - 2\gamma = 2\gamma(\cos\theta - 1), \tag{29}$$

derived from a mechanical balance of a film and the adjacent meniscus at the contact line, assuming the $\Pi\tau$

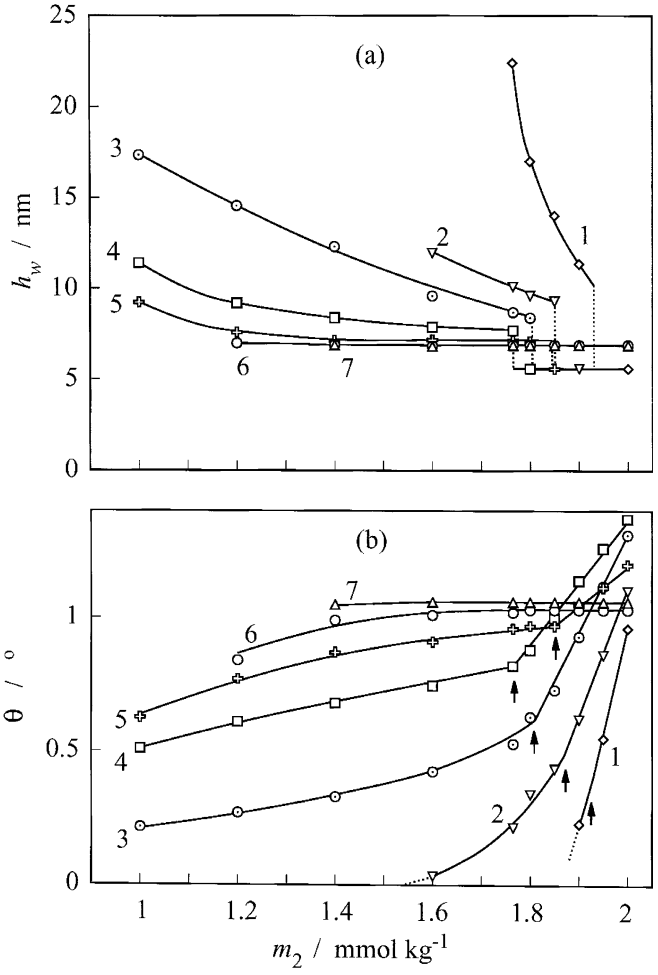

Fig. 4a, b Equivalent film thickness vs. molality of DeMS curves (**a**), and contact angle vs. molality of DeMS curves at constant NaCl concentration (**b**): *1* $m_1 = 5$ mmol kg^{-1}, *2* 10 mmol kg^{-1}, *3* 20 mmol kg^{-1}, *4* 40 mmol kg^{-1}, *5* 60 mmol kg^{-1}, *6* 80 mmol kg^{-1}, *7* 100 mmol kg^{-1}

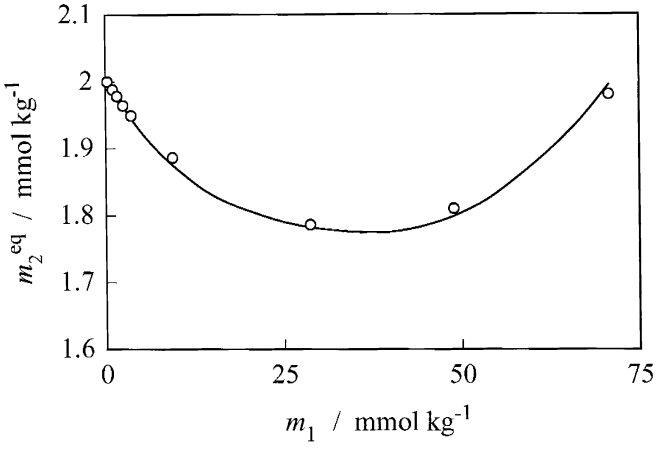

Fig. 5 Molality of DeMS vs. molality of NaCl curve at phase transition

term in Eq. 64 in Part I is negligible [8]. The calculated values of $\gamma^f - 2\gamma$ are shown as functions of m_1 and m_2 in Fig. 6 and Fig. 7, respectively. Typical errors in tension difference arising from the one in $\theta$are also shown for the curves of $m_2 = 1.9$ mmol kg^{-1} and $m_1 = 20$ mmol kg^{-1}. It is noticed that γ^f is smaller than 2γ and their difference is three orders of magnitude smaller than the γ and one order of magnitude less than that of SDS foam film [4]. Furthermore, the γ^f-2γ vs m_1 curve of higher m_2 in Fig. 6 has two breaks corresponding to the phase transitions, and exhibits a minimum in the region of Newton black film between the two breaks, and in Fig. 7, γ^f-2γ at lower m_1 decreases greatly with increasing m_2 in the region of Newton black film.

For symmetric films like foam films, formed from the aqueous solution of a binary mixture of uni-univalent electrolyte 1 and nonionic surfactant 2, we have

$$\nu_1 = 2,\ \nu_2 = 1, \tag{30}$$

and

$$\gamma_A = \gamma_B = \gamma,\ \Gamma_i^{H,A} = \Gamma_i^{H,B} = \Gamma_i^H,\ (i = 1,\ 2),\ \Delta y_A = \Delta y_B = \Delta y, \tag{31}$$

for Eq. 9 and Eq. 18, Eq. 19, Eq. 20, Eq. 21, Eq. 22, and Eq. 23. Then Eq. 10, Eq. 11, and Eq. 12 reduce to

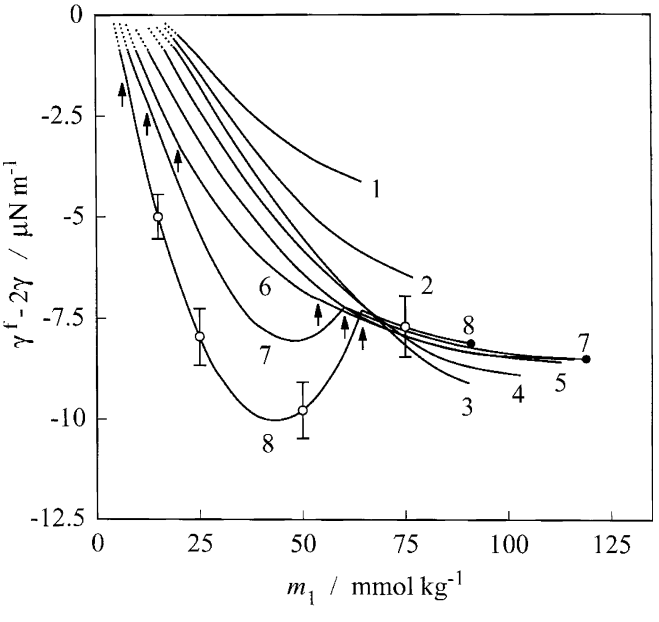

Fig. 6 Difference between film tension and surface tension vs. molality of NaCl curves at constant DeMS concentration: *1* $m_2 = 1$ mmol kg^{-1}, *2* 1.2 mmol kg^{-1}, *3* 1.4 mmol kg^{-1}, *4* 1.6 mmol kg^{-1}, *5* 1.765 mmol kg^{-1}, *6* 1.8 mmol kg^{-1}, *7* 1.85 mmol kg^{-1}, *8* 1.9 mmol kg^{-1}, *solid circles* γ^f-2γ at CMC of the NaCl-DeMS mixture

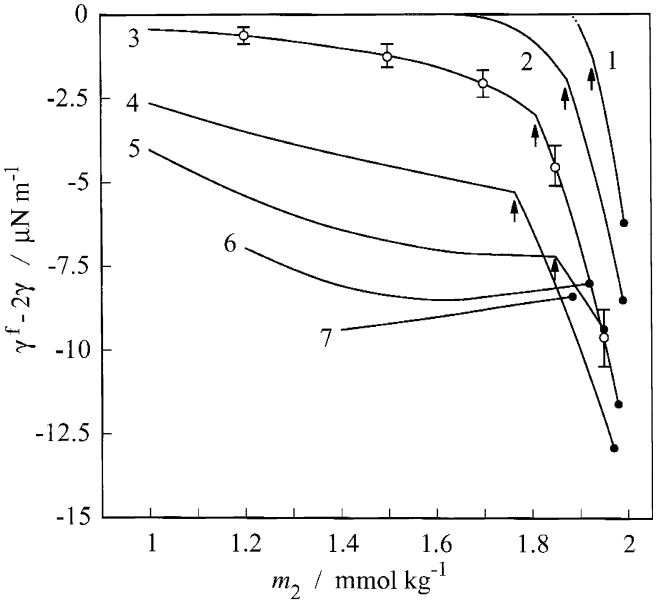

Fig. 7 Difference between film tension and surface tension vs. molality of DeMS curves at constant NaCl concentration: *1* $m_1 = 5$ mmol kg^{-1}, *2* 10 mmol kg^{-1}, *3* 20 mmol kg^{-1}, *4* 40 mmol kg^{-1}, *5* 60 mmol kg^{-1}, *6* 80 mmol kg^{-1}, *7* 100 mmol kg^{-1}, *solid circles* γ^f-2γ at CMC of the mixture

$$\frac{1}{2}\Gamma_1^f = \Gamma_1^F = \Gamma^F_{Na} + \quad = \Gamma^F_{Cl} - \ , \tag{32}$$

$$\frac{1}{2}\Gamma_2^f = \Gamma_2^F, \tag{33}$$

$$\frac{1}{2}\Delta y^f = \Delta y^F = y^F - \Gamma_1^F y_1 - \Gamma_2^F y_2, \tag{34}$$

and

$$\tau^f = v^L + 2\Gamma_1^F v_1 + 2\Gamma_2^F v_2, \tag{35}$$

where Γ_1^F and Γ_2^F are the surface densities of NaCl and DeMS at the film surface, respectively, Δy^F is the thermodynamic quantity change associated with the adsorption at the film surface and we have introduced

$$y_1 = y_{Na^+} + y_{Cl^-}. \tag{36}$$

Equation 22 and Equation 23 reduce to

$$\Gamma_1^F - \Gamma_1^H = -\frac{1}{4}(m_1/RT)\left[\partial\left(\gamma^f - 2\gamma\right)/\partial m_1\right]_{T,p,\Pi,m_2}, \tag{37}$$

and

$$\Gamma_2^F - \Gamma_2^H = -\frac{1}{2}(m_2/RT)\left[\partial\left(\gamma^f - 2\gamma\right)/\partial m_2\right]_{T,p,\Pi,m_1}, \tag{38}$$

respectively, assuming the aqueous solutions to be ideal.

The numerical values of $\Gamma_1^F - \Gamma_1^H$, obtained by applying Eq. 37 to the γ^f-2γ versus m_1 curve in Fig. 6 are plotted against m_1 together with the error in calculation at 1.9 mmol kg^{-1} in Fig. 8a. Figure 8b presents the Γ_1^H versus m_1 curve obtained from the surface tension measurement [9]. At lower m_2, Γ_1^F of a common black film is always larger than Γ_1^H, i.e., NaCl is richer in the adsorbed film of the common black film than in the one at the solution surface coexisting in equilibrium with the black film, which is consistent with the formation of a thinner film due to a reduction of electrostatic repulsion between the two surfaces in a film; surfaces of a DeMS foam film are negatively charged by the preferential adsorption of OH^- ions [19, 27]. The jump in Γ_1^F is observed for both the phase transitions from the common black to Newton black films at lower m_1 and from the Newton black to common black ones at higher m_1. The former is an ordinary transition due to the decrease in electrostatic double layer interaction

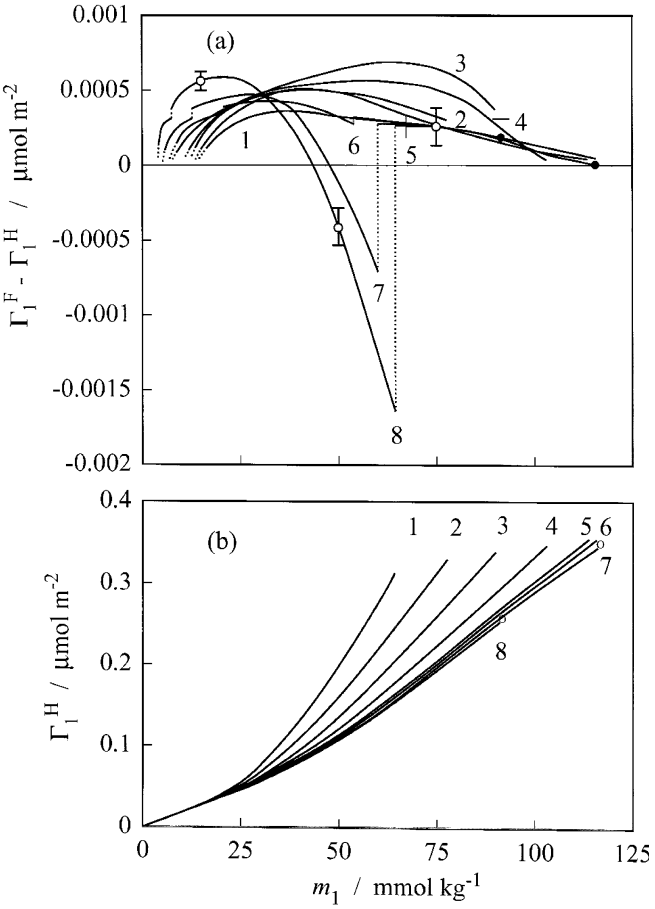

Fig. 8a, b Difference in surface density of NaCl vs. molality of NaCl curves (**a**) and surface density of NaCl at bulk surface vs. molality of NaCl curves at constant DeMS concentration (**b**): *1* $m_2 = 1$ mmol kg^{-1}, *2* 1.2 mmol kg^{-1}, *3* 1.4 mmol kg^{-1}, *4* 1.6 mmol kg^{-1}, *5* 1.765 mmol kg^{-1}, *6* 1.8 mmol kg^{-1}, *7* 1.85 mmol kg^{-1}, *8* 1.9 mmol kg^{-1}, *solid circles* $\Gamma_1^F - \Gamma_1^H$at CMC of the mixture, *open circles* Γ_1^H at CMC of the mixture

between the surfaces in a common black film, and the latter is probably caused by the large positive adsorption of NaCl at higher m_1 shown in Fig. 8b. $\Gamma_2^F - \Gamma_2^H$, numerically evaluated by fitting Eq. 38 to the γ^f-2γ versus m_2 curve in Fig. 7, is shown as a function of m_2 in Fig. 9. It is seen that the Γ_2^F value of the common black film is similar to the Γ_2^H value, but that of the Newton black film is larger than the Γ_2^H, that is, DeMS is enriched more in the adsorbed film of the Newton black film than that of the common black film. Such a behavior is also observed for the SDS foam film [4]. To elucidate the effect of added NaCl on the adsorption of DeMS at the film surface, the $\Gamma_2^F - \Gamma_2^H$ value at a given m_2 taken from Fig. 9 and the Γ_2^H value [9] are plotted against m_1 in Fig. 10a and b, respectively. Figure 10a shows that the $\Gamma_2^F - \Gamma_2^H$ of the Newton black film is larger than that of the common black film and decreases with an increase in m_1. From the comparison between Fig. 8a and Fig. 10a, it is noticed that the $\Gamma_1^F - \Gamma_1^H$ is much smaller than the $\Gamma_2^F - \Gamma_2^H$. Furthermore, the increases in $\Gamma_1^F - \Gamma_1^H$ and $\Gamma_2^F - \Gamma_2^H$ at the first transition from the common black to Newton black films are qualitatively consistent with the corresponding ones of the SDS system [4]; however, the $\Gamma_1^F - \Gamma_1^H$ of the DeMS system is two orders of magnitude smaller than that of the SDS system whereas the magnitude of $\Gamma_2^F - \Gamma_2^H$ is of the same order for both systems. Hence the first transition is attributable to the enhanced adsorption of surfactant caused by the positive adsorption of NaCl. On the other hand, the second transition at higher m_1 is accompanied by an increase in Γ_1^F and a decrease in Γ_2^F, whereas the first one at lower m_1 is accompanied by an increase both in Γ_1^F and Γ_2^F, as shown in Fig. 8a and Fig. 10a. Let us examine how the change in Γ_2^F at the transition affects the van der Waals attraction between the film surfaces by assuming the Hamaker function is simply proportional to the square of Γ_2^F[14, 28]. For $m_2 = 1.9$ mmol kg^{-1}, the increase in Γ_2^F by 0.008 μmol m^{-2} at the first transition enhances the van der Waals component Π_v of disjoining pressure by 40 Pa and the decrease by 0.0074 μmol m^{-2} at the second transition reduces Π_v by 12 Pa in the Newton black film (see Appendix III). Although the changes in Γ_2^F at the transitions is small, the resultant changes in Π_v are significant because they are comparable to the disjoining pressure which counterbalances the constant

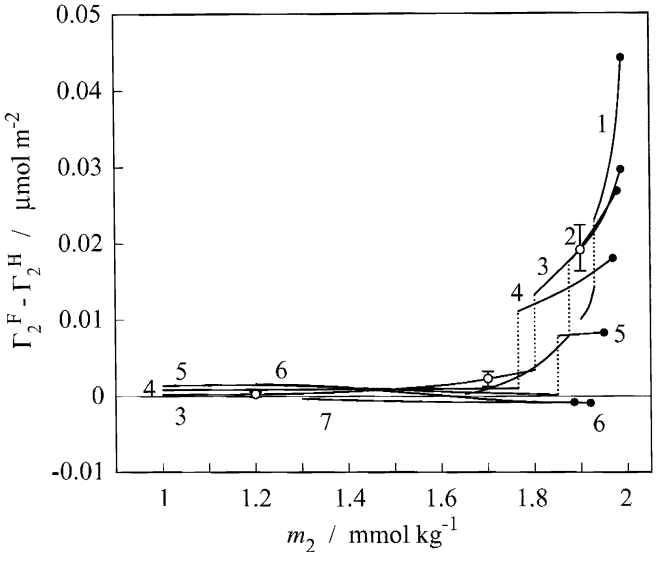

Fig. 9 Difference in surface density of DeMS vs. molality of DeMS curves at constant NaCl concentration: *1* $m_1 = 5$ mmol kg^{-1}, *2* 10 mmol kg^{-1}, *3* 20 mmol kg^{-1}, *4* 40 mmol kg^{-1}, *5* 60 mmol kg^{-1}, *6* 80 mmol kg^{-1}, *7* 100 mmol kg^{-1}, *solid circles* $\Gamma_2^F - \Gamma_2^H$ at CMC of the mixture

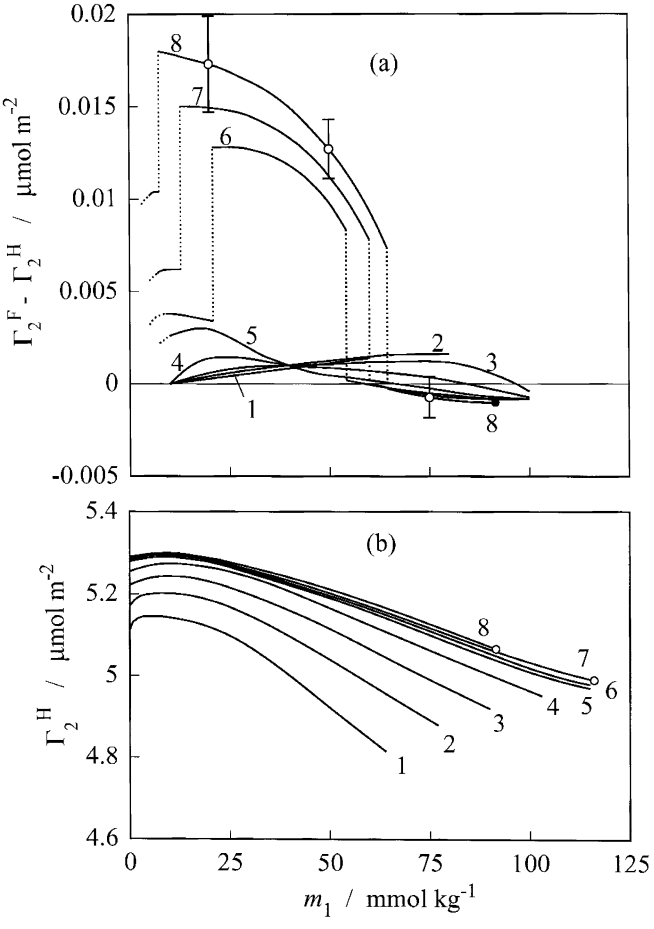

Fig. 10a, b Difference in surface density of DeMS vs. molality of NaCl curves (**a**) and surface density of DeMS at bulk surface vs. molality of NaCl curves at constant DeMS concentration (**b**): *1* $m_2 = 1$ mmol kg^{-1}, *2* 1.2 mmol kg^{-1}, *3* 1.4 mmol kg^{-1}, *4* 1.6 mmol kg^{-1}, *5* 1.765 mmol kg^{-1}, *6* 1.8 mmol kg^{-1}, *7* 1.85 mmol kg^{-1}, *8* 1.9 mmol kg^{-1}, *solid circles* $\Gamma_2^F - \Gamma_2^H$ at CMC of the mixture, *open circles* Γ_2^H at CMC of the mixture

capillary pressure of 30 Pa in the system. Hence, taking the large increase in the surface adsorption of NaCl in Fig. 8b and the decrease in the one of DeMS in Fig. 10b at higher m_1 into consideration, we conclude that the second transition is caused by the large adsorption of NaCl and the reduced adsorption of DeMS; the former enhances double layer repulsion in a manner similar to the adsorption of Ca^{2+} ions onto phospholipid monolayers [23, 24, 25], and the latter weakens van der Waals attraction between the surfaces in the Newton black film and the both induce the second phase transition to common black film.

Conclusions

1. Combination of the thermodynamic study of thin liquid films in Part I of this series with that of interfaces based on the Hansen convention enables us to clarify the structure and property of thin liquid films, the phase transition in the film, and the difference in thermodynamic quantity between the film interface and the bulk one.
2. The black foam film stabilized by DeMS in the presence of NaCl is stable at concentrations above one-half of the CMC of DeMS and the Newton black film is observed only above 1.765 mmol kg^{-1}, the critical molality of DeMS.
3. The phase transition in the black film is accompanied by the jump in equivalent film thickness and the break on the contact angle versus concentration curve, and depends on the molality of DeMS as well as that of NaCl.
4. The equivalent film thickness of the Newton black film of DeMS is 5.6 nm at 298.15 K and 30 Pa under atmospheric pressure, which is independent both of the molalities of NaCl and DeMS.
5. The phase transition takes place twice as the molality of NaCl increases at constant molality of DeMS: the first is the usual one from the common black to Newton black films caused by the increase both in the surface densities of NaCl and DeMS at the film surfaces, and the second is from the Newton black to common black films due to the large increase in the surface density of NaCl and the decrease in the surface density of DeMS.
6. The molality of NaCl at which the first transition from the common black to Newton black film takes place is two orders of magnitude smaller for DeMS than for ionic surfactants.

Appendix I

For a symmetric film, we have A = B in Part I of this series. Total number of components in the system is $c+3$; a and l denote the solvents in the phases A and L, respectively and 1,..., c the solutes. According to the surface excess convention for thin liquid films and the Gibbs convention for interfaces, the total differentials of film tension and the surface tension in the system are expressed by

$$\mathrm{d}\gamma^{\mathrm{f}} = -2s^{\mathrm{f}}\mathrm{d}T + h\mathrm{d}\Pi - 2\Gamma_a\mathrm{d}\mu_a - 2\sum_{i=1}^{c}\Gamma_i\mathrm{d}\mu_i \tag{I.1}$$

and

$$\mathrm{d}\gamma = -s^{\mathrm{G}}\mathrm{d}T - \Gamma_a^{\mathrm{G}}\mathrm{d}\mu_a - \sum_{i=1}^{c}\Gamma_i^{\mathrm{G}}\mathrm{d}\mu_i, \tag{I.2}$$

where s^{f} and s^{G} denote the excess entropy per unit surface area at the film surface based on the surface excess convention and the one at the adjacent meniscus based on the Gibbs convention respectively [6], and h is the distance between the two dividing planes for the film which make the surface excess of solvent $l$to be zero. Equations 2 and 4 in Part I can be rewritten by

$$c_a^{\mathrm{A}}\mathrm{d}\mu_a + c_l^{\mathrm{A}}\mathrm{d}\mu_l = -s^{\mathrm{A}}\mathrm{d}T + \mathrm{d}p - \sum_{i=1}^{c}c_i^{\mathrm{A}}\mathrm{d}\mu_i \tag{I.3}$$

and

$$c_a^{\mathrm{L}}\mathrm{d}\mu_a + c_l^{\mathrm{L}}\mathrm{d}\mu_l = -s^{\mathrm{L}}\mathrm{d}T + \mathrm{d}p - \mathrm{d}\Pi - \sum_{i=1}^{c}c_i^{\mathrm{L}}\mathrm{d}\mu_i, \tag{I.4}$$

respectively. Eliminating $\mathrm{d}\mu_1$ between Eq. I.3 and Eq. I.4 yields

$$\mathrm{d}\mu_a = D^{-1}\left(-D_s\mathrm{d}T + D_v\mathrm{d}p - D_{\mathrm{L}}\mathrm{d}\Pi - \sum_{i=1}^{c}D_i\mathrm{d}\mu_i\right), \tag{I.5}$$

where D, D_S, D_v, D_L, and D_i are the determinants:

$$D = \begin{vmatrix} c_a^{\mathrm{A}} & c_l^{\mathrm{A}} \\ c_a^{\mathrm{L}} & c_l^{\mathrm{L}} \end{vmatrix},\ D_S = \begin{vmatrix} s^{\mathrm{A}} & c_l^{\mathrm{A}} \\ s^{\mathrm{L}} & c_l^{\mathrm{L}} \end{vmatrix},\ D_v = \begin{vmatrix} 1 & c_l^{\mathrm{A}} \\ 1 & c_l^{\mathrm{L}} \end{vmatrix},\ D_L = \begin{vmatrix} 0 & c_l^{\mathrm{A}} \\ 1 & c_l^{\mathrm{L}} \end{vmatrix},\ D_i = \begin{vmatrix} c_i^{\mathrm{A}} & c_l^{\mathrm{A}} \\ c_i^{\mathrm{L}} & c_l^{\mathrm{L}} \end{vmatrix},\ (i = 1, \ldots, c). \tag{I.6}$$

Substitution of Eq. I.5 into Eq. I.1 and Eq. I.2 leads to

$$\mathrm{d}\gamma^{\mathrm{f}} = -2\left[s^{\mathrm{f}} - \Gamma_a(D_S/D)\right]\mathrm{d}T - 2\Gamma_a(D_v/D)\mathrm{d}p + \left[h + 2\Gamma_a(D_{\mathrm{L}}/D)\right]\mathrm{d}\Pi - 2\sum_{i=1}^{c}\left[\Gamma_i - \Gamma_a(D_i/D)\right]\mathrm{d}\mu_i \tag{I.7}$$

and

$$d\gamma = -\left[s^G - \Gamma_a^G(D_S/D)\right]dT - 2\Gamma_a^G(D_v/D)dp + \Gamma_a^G(D_L/D)d\Pi - \sum_{i=1}^{c}\left[\Gamma_i^G - \Gamma_a^G(D_i/D)\right]d\mu_i. \quad (1.8)$$

Hence we can obtain Eq. 3 and Eq. 4 from Eq. I.7 and Eq. I.8.

Appendix II

For a given solution whose surface tension is γ_1, first R is tentatively determined by using Eq. 24 at $r = 0$

$$\Pi = 2\gamma_1/R. \quad (II.1)$$

R should be

$$R > 2\gamma_1/\Pi \quad (II.2)$$

because Πincreases with increasing r at constant R as shown in Eq. 24. Once we decide R_1 which satisfies Eq. II.2, r is determined by solving Eq. 24 for r

$$r = R_1\sqrt{1 - (2\gamma_1/R_1\Pi)}. \quad (III.3)$$

For instance, if $\Pi = 30$ Pa and $\gamma_1 = 30$ mN m^{-1}, $R > 2$ mm from Eq. II.2, we select the ring cell of $2R_1 = 4.5$ mm. Then $r = (4.5/2)\sqrt{1 - (4/4.5)} = 0.75$ mm.

Practically, the r versus $\hat{m}$ curve at constant $\hat{X}_2$ was obtained at $\Pi = 30$ Pa for a given R since the γ versus $\hat{m}$ curve is known in the previous study [9] and the r versus $\hat{m}$ curve obtained for each R was used as a calibration curve.

Appendix III

We calculate only the Π_v for the common black and Newton black films because the electric potential of diffuse double layer in Newton black film and the short-range non-DLVO interaction are not explicitly known. Π_v is given by

$$\Pi_v = -A^*/6\pi h^3 \quad (III.1)$$

where A^* is the composite Hamaker function for the film [14] and h the real physical film thickness. The A^* values were taken from [14] and h was calculated from h_w using

$$h = h_w + 2h_2\left[(n_1)^2 - (n_2)^2\right]/\left[(n_1)^2 - 1\right] \quad (III.2)$$

[29] and assuming the thickness h_2 of hydrocarbon layer in the adsorbed film to be 1.41 nm and the refractive indices n_1 and n_2 of aqueous core and hydrocarbon layer to be 1.334 and 1.412 at 298.15 K for the DeMS film, respectively.

For $m_2 = 1.9$ mmol kg^{-1}, numerical values of Γ_2^F and h_w at the transition points were read from Fig. 10 and Fig. 3. Then, at the first transition, $\Gamma_2^F = 5.31\,\mu$mol m^{-2}, $h = 8.78$ nm, and $A^* = 0.4\times10^{-20}$ J lead to $\Pi_v = -31.4$ Pa for the common black film and 5.318 μmol m^{-2}, 4.83 nm, and 2.8×10^{-20} J to -1.32×10^4 Pa for the Newton one; at the second transition, 5.1724 μmol m^{-2}, 4.83 nm, and 2.65×10^{-20} J lead to -1.25×10^4 Pa for the Newton one and 5.165 μmol m^{-2}, 6.33 nm, 2.0×10^{-20} J, and -4.19×10^3 Pa for the common one. Assuming that A^* is proportional to $\left(\Gamma_2^F\right)^2$, it was found that the increase in Γ_2^F by 0.008 μmol m^{-2} at the first transition enhances the van der Waals component of disjoining pressure in the Newton black film by 40 Pa, and the decrease by 0.0074 μmol m^{-2} at the second transition reduces the Π_v by 12 Pa in the Newton black film.

References

1. Rusanov AI (1971) Thermodynamics of films. In: Derjaguin BV (ed) Research in Surface Forces, vol 3. Consultants Bureau, New York, pp 103–110
2. Toshev BV, Ivanov IB (1975) Colloid Polym Sci 253:558
3. Ivanov IB, Toshev BV (1975) Colloid Polym Sci 253:593
4. de Feijter JA, Vrij A (1978) J Colloid Interface Sci 64:269
5. Toshev BV (1981) Colloids Surf 2:243
6. de Feijter JA (1988) Thermodynamics of thin liquid films. In: Ivanov IB (ed) Thin Liquid Films, Surfactant Science Series 29, Dekker, New York, Chap 1
7. Motomura K, Iwanaga S, Hayami Y, Uryu S, Matuura R (1981) J Colloid Interface Sci 80:32
8. Iyota H, Krustev R, Müller H-J (in press) Colloid Polym Sci
9. Iyota H, Tomimitsu T (2003) J Colloid Interface Sci 257:327
10. Jones MN, Mysels KJ, Scholten PC (1966) Trans Faraday Soc 62:1336
11. Scheludko A (1967) Adv Colloid Interface Sci 1:391
12. Kolarov T, Cohen R, Exerowa D (1989) Colloids Surf 42:49
13. Müller H-J, Rheinländer T (1996) Langmuir 12:2334
14. Clunie JS, Corkill JM, Goodman JF, Ingram BT (1970) Spec Discuss Faraday Soc 1:30
15. Ingram BT (1972) J Chem Soc Faraday Trans 1 68:2230
16. Krustev R, Müller H-J, Toca-Herrera JL (1998) Colloid Polym Sci 276:518
17. Scheludko A, Radoev B, Kolarov T (1968) Trans Faraday Soc 64:2213
18. Kolarov T, Scheludko A, Exerowa D (1968) Trans Faraday Soc 64:2864
19. Exerowa D, Zacharieva M, Cohen R, Platikanov D (1979) Colloid Polym Sci. 257:1089

20. Iyota H, Shimada K, Abe K, Ikeda N, Motomura K, Aratono M (2001) J Colloid Interface Sci 234:322
21. Kolarov T, Exerowa D, Krumova Zh, Rangelova N (1974/75) Ann Univ Sofia, Fac Cem 69:99
22. Exerowa D (1978) Commun Dept Chem Bulg Acad Sci 11:739
23. Cohen R, Exerowa D, Koralov T, Yamanaka T, Muller VM (1992) Colloids Surf 65:201
24. Yamanaka T, Tano T, Kamegawa O (1994) Langmuir 10:1871
25. Cohen R, Exerowa D, Yamanaka T (1996) Langmuir 12:5419
26. Exerowa D, Kruglyakov PM (1998) Foam and foam films, studies in interface science ser. 5. Elsevier, Amsterdam, Chap 3
27. Manev ED, Pugh RJ (1991) Langmuir 7:2253
28. Israelachvili JN (1992) Intermolecular and surface forces, 2nd edn. Academic, London, Chap 11
29. Frankel SP, Mysels KJ (1966) J Appl Phys 37:3725